RESEARCH PAPER

Experimental analysis of the effect of gas flow rate and nature on plasma arc cutting of hardox-400

Deepak Kumar Naik[1] · Kalipada Maity[2]

Abstract
This research paper exhibits an experimental investigation of plasma arc cutting of hardox-400 using different types of plasma gases. Nature and behavior of the plasma arc were studied and described the effect of plasma gas on the workpiece. The experiments were performed on 10 mm hardox-400 using CNC plasma cutting machine. The selected workpiece material has very good mechanical properties like high toughness, good bendability, and good weldability. This special abrasion resistance steel is used in part manufacturing of front loaders, buckets, barges, and various mining equipment. Four different plasma gases were chosen for this experiment, i.e., air, argon, oxygen, and nitrogen. Thermophysical properties of plasma gases, properties of generated arc, cutting performance, and energy balance are explained for different plasma gases used. The kerf shape and material removal rate (MRR) due to the generated arc were measured and analyzed the effect. This paper clarifies the potential of cutting process by varying the flow rate and chemical composition of the plasma gas.

Keywords Hardox-400 · Kerf energy · Radial distance · Flow rate · Arc diameter

1 Introduction

Modern manufacturing industries emphasize on accurate cutting of materials plate due to high demand in the industrial sector. Previously oxy-fuel cutting process was employed to cut the plate material. But, the production rate was affected due to its poor dimensional accuracy and slower cutting speed. Plasma arc cutting (PAC) process is introduced to overcome this problem. This process also used to cut high strength material which is very difficult to cut in oxy-fuel cutting process. The only limitation of the process is the cutting material should be conductive in nature. Better flexibility and faster

✉ Kalipada Maity
kpmaity@gmail.com

Deepak Kumar Naik
naikdeepak81@gmail.com

[1] Department of Mechanical Engineering, Sree Vidyanikethan Engineering College(Autonomous), Tirupati, Andhra Pradesh 517102, India

[2] Department of Mechanical Engineering, National Institute of Technology Rourkela, Rourkela, Odisha 769008, India

productivity at cheaper cost are the prime advantages of PAC over other cutting process [1].

PAC process involves the thermal cutting phenomena in which plasma gas is applied to cut the material. Plasma is a fourth state of matter. If substantial heat energy added to the gaseous medium, it gets ionized and behaves like a highly energized gas. PAC applies high velocity plasma jet to melt and remove the material from the workpiece [2]. Higher amount of current is applied to generate the plasma channel between the workpiece and electrode. The temperature of plasma reaches around 20,000 °C due to supply of high current [3]. High strength alloy can be cut through this cutting process. Hardox-400 (EN 10029) is a special type of abrasion resistance steel which is nearly three times harder than normal steel. This material has superior mechanical properties, i.e., good bendability, good weldability, and high toughness. This alloy material is used to manufacture the parts which associate with construction, mining, and drilling industries.

In PAC process, initially argon and nitrogen gases were used as primary gas for generation of plasma. In 1960, to achieve the cut quality of the surface and higher cutting speed, air plasma was introduced. Oxygen plasma increases the quality of cut due to its oxidizing properties [4, 5]. Arc current under 100 A is available in the market for air cutting. Oxygen, nitrogen, and air were used as plasma gas in various research

work. The selection of the plasma gas depends on the work-piece material to be cut [6–10]. Kavka et al. [11] studied the PAC process using three different gases and one liquid media as plasma gas, i.e., oxygen, air nitrogen, and steam. They explained the effect of gas nature and flow rate on mild steel material. Ramakrishnan et al. [12] investigated the properties of produced plasma using different gas. They made a relation between flow rate of plasma gas and the diameter of torch nozzle. An investigation was presented on properties of plasma produced from the air cutting [13]. Research and development on PAC process are devoted to correlation between cutting performance and arc properties [14, 15], phenomena of electrode [16]. Nemchinsky and Severance [17] studied the phenomena of kerf width generated using PAC process and introduced a model that affects the cut quality. Gonzalez et al. [18] characterized the generated plasma with energy transferred using argon as a plasma gas. Long et al. [19] investigated experimentally and numerically the effect of cathode diameter in PAC process using process parameters such as gas flow rate, gas pressure, and cutting current. Ramakrishnan et al. [20] made a comparison of cut quality with oxygen, air, and nitrogen as plasma gas. But they focused on presence of oxygen on the kerf and overall energy balance.

The above literature study reports that the very less work has been done to obtain the effect of gas nature and flow rate of PAC process. This research work focuses on the properties of produced arc using four plasma gases and their effect on cutting performance and energy balance. The analysis of aforementioned responses can be useful for research and development sector of various industries. This paper also compares the kerf width with nitrogen, air, oxygen, and argon as a plasma gas.

2 Experimental procedure

The experiments were performed on computer numerical controlled (CNC) plasma arc cutting machine (Burny 1205) of MESSER company. The photograph of the machine is shown in Fig.1. Air cooled type swirl nozzle of copper material having 2 mm diameter was taken for the experiment. Tungsten electrode with hafnium insertion used in plasma torch. The shielding gas was not used for cooling purpose in this study. Air was selected as a cooling medium to prevent the excessive heating while generation of plasma. The gas supply was arranged in to the torch body through centrally connected pipe and adjusted by controllers.

The power supply was arranged in such a manner that the current may be increase up to 70 A. For all the experiments, the intensity of current was kept constant at 70 A. Only two process parameters were varied, i.e., flow rate and type of plasma gas, during the operations. For all study, the flow rate of plasma gas was varied between 8 g/min and 16 g/min. The input parameters are shown in Table 1. Argon, nitrogen,

Fig. 1 CNC PAC machine

oxygen, and air were used as plasma gas. The selection of plasma gas involves a major role in the cutting process. Therefore the gases were selected according to the previous literature study [11].

The pressure was measured inside the arc chamber of the plasma torch body. The schematic diagram of plasma arc chamber is shown in Fig.2. The flow rate of plasma medium was controlled with the help of control valve which is mounted in the inlet of pipe. The measurements extract a strong relationship between chamber pressure and flow rate which is portrayed in Fig.3. It shows the trend that, increase in gas flow rate increases the chamber pressure inside the torch body.

During the experiments, the torch body was arranged as a moving system which direction was controlled by the CNC machine. The work piece was fixed at the same position. Cutting speed and standoff distance were also kept constant during the experiments as 30 cm/min and 2 mm, respectively. The kerf width was measured using digital vernier caliper from the cut edge of the surface. The upper jaw for inside measurement was inserted in the gap of kerf width and noted the reading.

The whole experiments were performed on AR 400(EN 10029) of sheet thickness of 10 mm. The chemical composition of the material is shown in Table 2. Also, the material properties of the same material are tabulated in Table 3.

Heat capacity of iron depends on the temperature in the solid phase, while it does not depend in liquid phase for the temperature range considered in this work [22]. So, the

Table 1 Input parameters

Input Parameters	Ranges
Types of plasma gases	Air, Argon, Oxygen, Nitrogen
Cutting current (A)	70
Flow rate of plasma gas (g/min)	8,10,12,14,16

Fig. 2 Plasma arc chamber
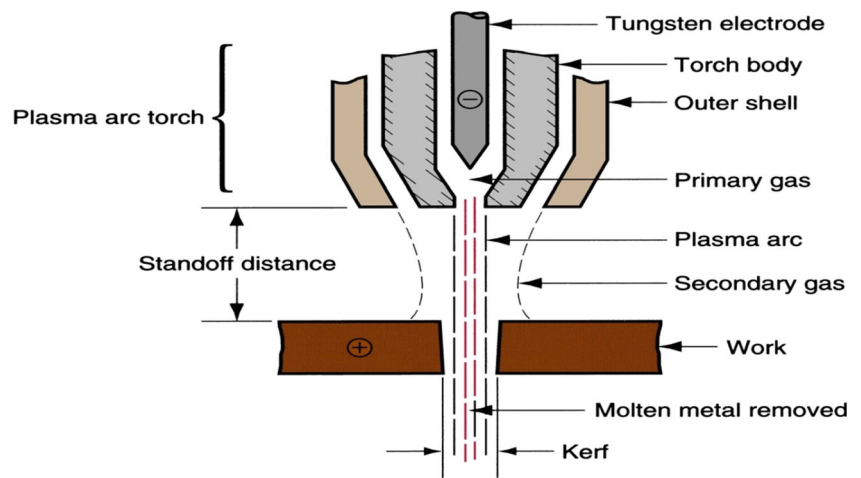
average value for the whole temperature was considered in this paper.

Charged coupled device (CCD) was used to take the images of the arc column. The arc column diameter was estimated from those images. Average values of the same were considered for calculation of radial intensity.

The thermophysical properties were calculated of the pressure of 1–3 atm and temperature ranges between 4000 K and 35,000 K for the gases used in this experiment. By using classical methods, thermodynamic properties and equilibrium composition were determined. Standard formulae were used to compute the equilibrium thermodynamic properties of mass density, enthalpy, sound velocity, and heat capacity for each pressure. The Boltzmann equation describes the statistical behavior of a thermodynamic system. Chapman–Enskog method provides a framework in which equations of hydrodynamics for a gas can be derived from that Boltzmann equation. So, this method was applied to calculate the transport coefficient. The fourth approximation of Boltzmann equation was used for this manuscript. The applied method described in detail in [23]. Figs. 4,5,6 show the temperature dependence of enthalpy, temperature of electrical conductivity, and speed of sound velocity of used gases for 1 atm pressure. From the

Fig. 3 Gas flow rate versus chamber pressure

above figures, it is obtained that increase in pressure increases the gas density and directly proportional with pressure. Moreover, the thermophysical properties are less affected by pressure. Decrease in pressure slightly decreases the speed of sound and enthalpy for temperature ranges 13,000 K and 24,000 K. Further, above 25,000 K, pressure is significant for dependence of electrical conductivity.

3 Result and discussion

3.1 Generated plasma arc properties

The relation between the chamber pressure and the arc voltage is shown in Fig. 7. The voltage drop between the nozzle and cathode was recorded for plasma gases used in this work. From the Fig. 7, it is found that the increase in pressure increases the voltage. The argon gas generates the higher voltage comparing to the other gases used in this experiment due its high specific enthalpy. Convection is the dominant process during distribution of energy [24]. So, the cutting arc comes with strong axial flow types of arc. The electric field intensity is calculated by $E = \sqrt{\frac{H}{\sigma}}$, where "H" and "σ" represent the plasma enthalpy and the electrical conductivity corresponding [23]. Electrical conductivity plays a vital role for temperature rather than plasma gas, where enthalpy depends on both the aforesaid parameter. Comparing to other gases, argon is the much higher enthalpy at the same temperature. This is due to reaction enthalpy which breaks the molecular bonds and ionization, an example taken for the brief description of the above statement. One molecule of water splits into three atoms, whereas in case of ethanol, it breaks into nine atoms. Due to this higher enthalpy explains higher voltage because of ionization at higher temperatures. Thus, higher enthalpy creates higher amount of voltage. Oxygen enthalpy measures lower voltage as compared to other plasma gases studied. There is no major difference between air and nitrogen, whereas argon
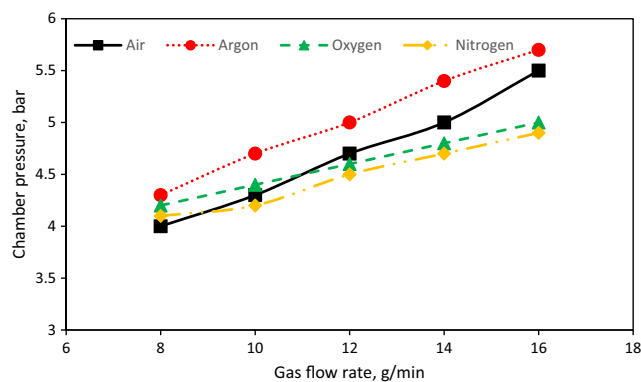
Table 2 Chemical composition of hardox-400 [21]

Material	Elements									
	C P	C	S	Mn	Si	Cr	Ni	B	Mo	Fe
Hardox-400	0.025	0.015	0.01	1.6	0.7	0.5	0.25	0.004	0.25	Balance

creates more voltage difference in increasing range of chamber pressure.

Aubrecht and Bartlove [25] evaluated the effect of gas flow using radial intensity dependence on pressure. Figure 8 shows the relation between radial intensity and radial distance of flow rate of plasma medium for 12 g/min at the torch exit. From this figure, nitrogen, argon, and air unveil sharp profiles, whereas oxygen exhibits faster drop on edges. When there is no radial distance, there is maximum radial intensity. Oxygen gas produces lower intensity comparing to other gases.

The relation between plasma gas flow rate and dependence of arc diameter is portrayed in Fig. 9. The arc diameter was measured and found that the values were lesser than the diameter of nozzle ($d < 1$ mm). There are two flow zones during the nozzle openings, i.e., outer cold zone and hot conducting zone [13, 20]. The temperature is lower in the outer zone as compared to hot conducting zone to sustain significant ionization. Maximum energy transferred occurs at the hot zone. Thus, mass flux density is bigger in the cold zone. The arc diameter decreases in increase of gas flow rate for all the studied gases in this experiment. The widest arc diameter was found for oxygen and lowest for air plasma. Higher arc constriction found at smaller arc diameter, which increases the nozzle voltage and electric field.

Figure 10 shows the temperature profiles for all different studied gases at the nozzle exit at a constant flow rate of plasma gases. Girard et al. [4] presented the temperature profiles for an oxygen plasma working on the same arc current, and all gases provide the temperatures around 23,000⁰ K in the same region. The flow corresponds to the sonic region for all profiles. The temperature was smallest for argon and largest for the nitrogen arcs. The temperature of the arc for the centerline for different flow rates at the torch exit is shown in Table 4. For oxygen plasma gas, the centerline temperature increases significantly, and for other gases, it does not depend on the gas flow rate.

Table 3 Material properties of hardox-400 [21]

Thermal conductivity (W/mK)	40
Density (kg/m)	9410
Melting point (K)	3000
Yield strength (Mpa)	950
Hardness (HBW)	390

3.2 Performance of cutting

Figure 11 shows the kerf geometries on the workpiece for different plasma gases used. The appearance of kerf width with nitrogen is very similar to air because air contains 79% of nitrogen. The kerf is narrow toward the bottom and wider at the top. However, other two used gases reveal similar types of kerf which is narrowest at the top and bottom. The central portion of the kerf is little bit widen compared to the top and bottom portion. From the above result, it disclosed that the kerf width is not uniform during cutting due to improper heat distribution along the kerf surface.

Bini et al. [26] found that the minimum stand-off-distance creates the kerf with negative inclination from the both sides. Whenever there is small arc diameter, the plasma enters on to the workpiece. However, at the same stand-off-distance, air and nitrogen cuts do not give such a feature. Nemchinsky [17] explained the reason behind the narrower kerf toward bottom. The kerf thickens toward the bottom of the plate due to separation of the layer from the solid metals..

During the plasma arc cutting, the material removal rate was calculated using the equation.
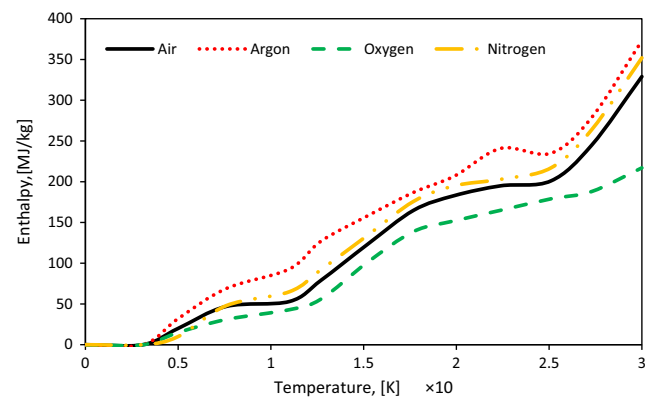
$$\eta = V \times \rho \times \int_0^h K(Z)dz$$

where $\rho =$ Density of the material.

$V =$ cutting speed.

$K(Z) =$ width of kerf.

The material removal rate (MRR) is the measurement for how much material is removed from a part in a given period of cutting or total volume removed from workpiece. The MRR is

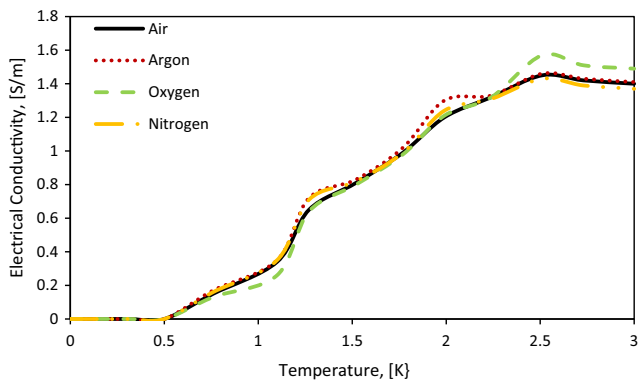

Fig. 4 Enthalpy versus Temperature for $P = 1$ atm

Fig. 5 Electrical conductivity versus Temperature for $P = 1$ atm

Fig. 7 Arc voltage versus chamber pressure

the product of cutting speed of the torch, density of the workpiece material, and kerf width which has obtained from plasma arc cutting process.

The kerf geometry is not uniform along the dimension. So, the integration was performed through the width of the kerf. The average value of the kerf width was taken for the calculation of MRR. The graph of calculated MRR versus gas flow rate for each plasma gas is shown in Fig. 12. From the graph, it is found that the oxygen and argon gas provide higher MRR. For air and nitrogen, increase in gas flow rate decreases the MRR. When flow rate increases, the constriction of arc also increases, and hence, the arc radius decreases. Maximum energy releases if supply of oxygen gas increases which causes higher MRR.

3.3 Energy balance of the PAC process

Teulet et al. [4] described the arc-material interaction. They applied and modified to compare energy terms for different gases involved in cutting process. The total electric energy is estimated by $Q_{el} = VI$, where "I" is the working current, "V" is the total voltage of arc, and "Q_{el}" is the total electric energy. There are some energy released during oxygen plasma gas cutting due to the oxidation with the material in the kerf. The oxidation is denoted by Q_{oxy}. The total energy is divided into four different constituents: energy losses above the plate
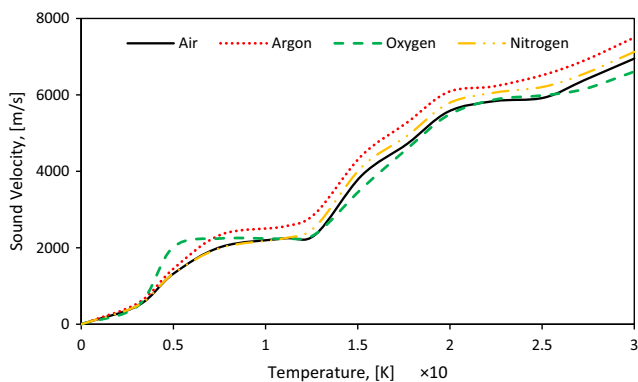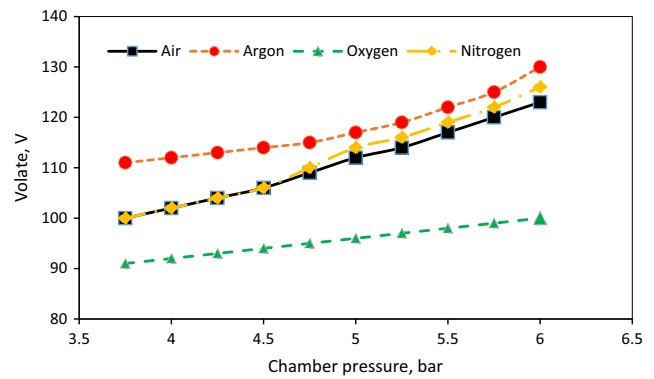
$Q_{lost-up}$, energy losses below the workpiece $Q_{lost-down}$, energy consumed for material removal from the kerf Q_{kerf}, and convective energy losses below the workpiece Q_{conv}. The total energy balance is evaluated by the following formulae:

$$Q_{oxy} + Q_{el} = Q_{lost-up} + Q_{lost-down+} Q_{kerf} + Q_{conv}$$

Energy losses above the plate represent the conduction, convection, and radiation losses between the top surface of the workpiece and the nozzle exit. The conduction and convection losses are very difficult to estimate in this part of arc. Thus, the radiation loss is estimated using this formula:

$$Q_{rad} = \pi Rs \times 4\pi\varepsilon_n \times z$$

where, "z" is the stand-off-distance, "R_s" radius of sphere plasma, and "ε_n" is the net emission coefficient.

Net emission coefficient calculation during plasma arc cutting process using nitrogen, air, and oxygen was established [25, 27]. Increase in arc radius decreases the radiation losses for stand-of-distance at 2 mm using different pressures. The radiation losses completely depend on the stand-of-distance. The temperature of plasma changes with stand-of-distance. The estimation shows the significance of the radiation losses.

The material gets heated, melted, and removed from the workpiece in kerf. Further, added heat energy to the molten material caused to leaving the kerf. Q_{kerf} is comprised of three constituents: energy required for fusion Q_m, energy required for heating the molten material Q_h, and energy needed for
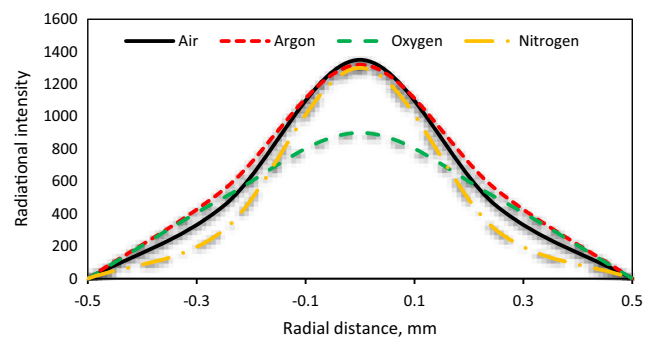

Fig. 6 Sound velocity versus Temperature for $P = 1$ atm

Fig. 8 Radial intensity versus radial distance for 12 g/min
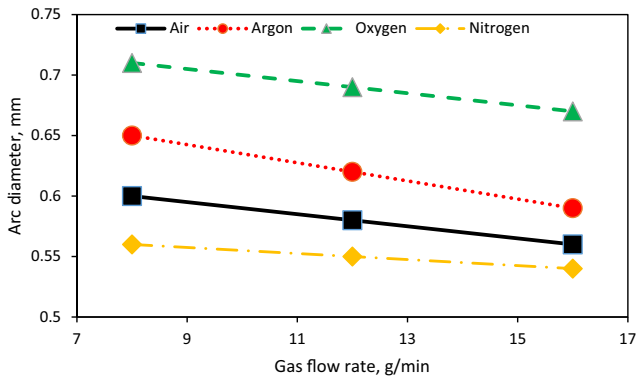
Fig. 9 Arc diameter versus gas flow rate

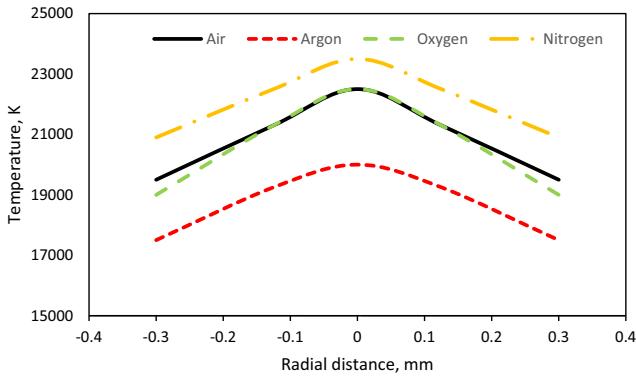Fig. 11 Kerf geometries on the workpiece

Fig. 10 Temperature versus radial distance

Fig. 12 MRR versus Gas flow rate

overheating the molten material Q_o. The total energy for heating the material is derived as $Q_h = M_m \times C_p \times (T_m-T_i)$, where T_i is the initial (room) temperature. Again, $Q_m = M_m \times L_f$. For estimating Q_o, material temperature inside the kerf is to determine.

Figure 13 shows the relation between measured temperature and gas flow rate. Air, nitrogen, and argon exhibit the similar nature, whereas oxygen behaves different nature comparing to other three. In case of oxygen gas, the temperature increases in increasing trend of gas flow rate. On the other
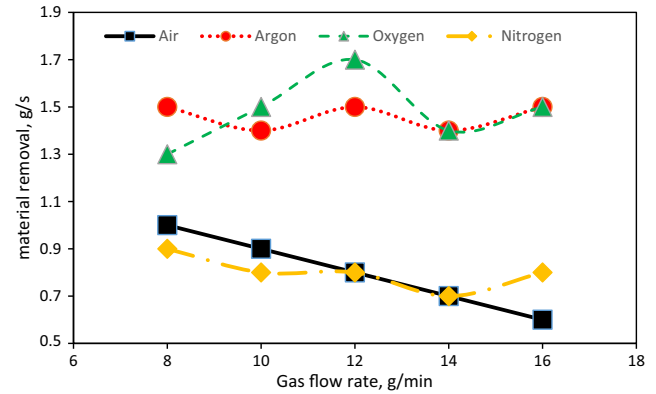
hand, while using other three gases, the temperature decreases in increasing trend of flow rate of plasma gas. The energy spent for material overheating was evaluated using average temperature value along the kerf.
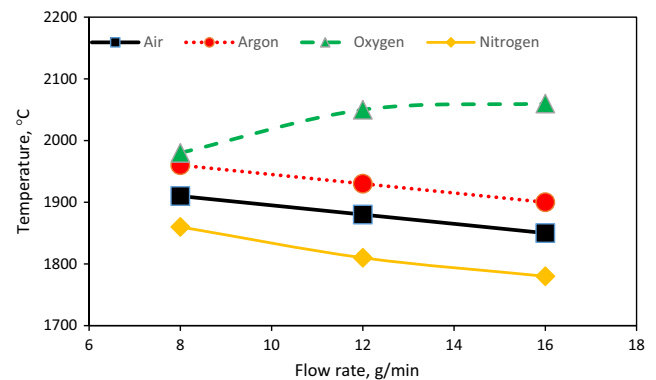
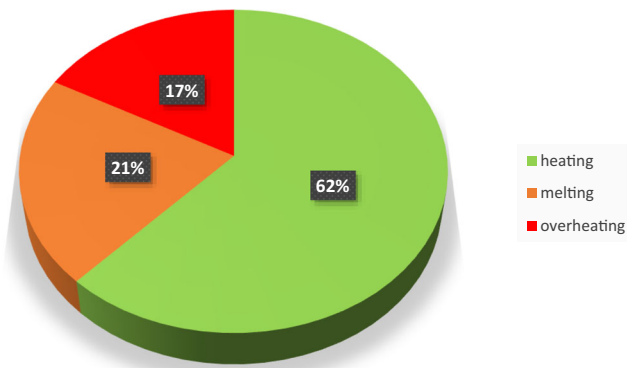$$Q_o = M_m \times C_p \times (T_{kerf}-T_{melt})$$

Table 4 Temperature of the arc for the centerline for different flow rates

Flow rate (g/min)	Axis temperature (K)			
	Argon	Oxygen	Nitrogen	Air
8	22,720	22,320	23,330	22,250
12	22,940	22,540	23,540	22,510
16	22,750	22,530	23,370	22,430

Fig. 13 Temperature versus Gas flow rate

Fig. 14 Percent constituent of the total energy consumed

Fig. 16 Conventional losses versus Gas flow rate

The percent component of the total energy spent is shown in Fig. 14. The energy consumed during heating the material to the melting point inside the kerf is presented. This energy is more than 60 % of the total kerf energy. About 21 % of energy was required to melting the material. The relation between the total energy spent inside the kerf and gas flow rate of studied gases is shown in Fig. 15. The energy decreases in increasing of gas flow rate in air and nitrogen gases. It behaves counterpart while using argon and oxygen as plasma gas. Oxygen exhibits the higher energy in higher amount of gas flow rate. The residual enthalpy measured after passing through the kerf is $Q_{lost-down}$. The graph between conventional losses and flow rate of plasma gas is shown in Fig. 16. The conventional losses increase with increase in gas flow rate for all the studied gases. The losses were highest for argon and lowest for nitrogen gas.

4 Conclusions

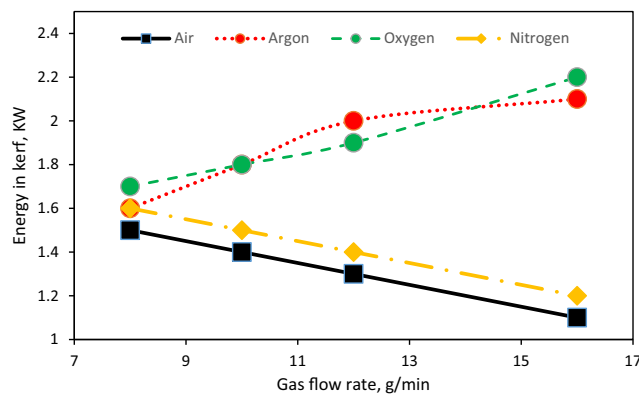The present research work exhibits the experimental study of the effect of plasma gas type and flow rate on hardox-400 material plate. Argon, air, nitrogen, and oxygen were used as plasma gas for cutting the aforesaid material. The following conclusions are drawn on the basis of the results of present investigation.

- The appearance of kerf width is very similar to while using nitrogen and air as a plasma gas in cutting process. Narrower kerf and smallest arc diameter can be achieved through these types of plasma gases.
- Wider kerf can be acquired in argon cutting due to higher energy density in the plasma gas. The radial heat transfer toward the material inside the kerf from the center is better in argon cutting.
- Higher material removal rate can be obtained using argon and oxygen as plasma gas. The maximum energy releases during cutting of material causes to higher material removal.
- The energy required to melt the material is 21% of the total energy and 61% energy used to heat the material inside the kerf.
- Higher cut quality during plasma arc cutting can achieved with higher gas flow rate because it increases both momentum density and energy.

Fig. 15 Total energy in kerf versus Gas flow rate

References

1. Gariboldi E, Previtali B (2005) High tolerance plasma arc cutting of commercially pure titanium. J Mater Process Technol 160(1):77–89
2. Nemchinsky VA, Severance W (2006) What we know and what we do not know about plasma arc cutting. J Phys D Appl Phys 39(22): R423
3. Maity KP, Bagal DK (2015) Effect of process parameters on cut quality of stainless steel of plasma arc cutting using hybrid approach. Int J Adv Manuf Technol 78(1–4):161–175
4. Girard L et al (2006) Experimental study of an oxygen plasma cutting torch: I. Spectroscopic analysis of the plasma jet. J Phys D Appl Phys 39(8):1543
5. Fernicola RC (1994) New oxygen plasma process rivals laser cutting methods. Welding Journal 73(6):65–69

6. Naik DK, Khan A, Majumder H, Garg RK (2019) Experimental investigation of the PMEDM of nickel free austenitic stainless steel: a promising coronary stent material. Silicon 11(2):899–907

7. Naik DK, Maity K (2018) Application of desirability function based response surface methodology (DRSM) for investigating the plasma arc cutting process of sailhard steel. World Journal of Engineering 15(4):505–512

8. Naik DK, Maity K (2019) Temperature analysis by moving heat source during plasma arc cutting process: an analytical approach. World Journal of Engineering 16(4):569–572

9. Naik DK, Maity K (2018) Optimization of dimensional accuracy in plasma arc cutting process employing parametric modelling approach. IOP Conference Series: Materials Science and Engineering 338:1–6

10. Naik DK, Maity K (2018) An optimization and experimental analysis of plasma arc cutting of Hardox-400 using Taguchi based desirability analysis. Materials Today: Proceedings 5(5):13157–13165

11. Kavka T et al (2013) Experimental study of the effect of gas nature on plasma arc cutting of mild steel. J Phys D Appl Phys 46(22):224011

12. Ramakrishnan S et al (1997) Plasma generation for the plasma cutting process. IEEE Transactions on plasma science 25(5):937–946

13. Ramakrishnan S, Rogozinski M (1997) Properties of electric arc plasma for metal cutting. J Phys D Appl Phys 30(4):636

14. Freton P et al (2001) Numerical and experimental study of a plasma cutting torch. J Phys D Appl Phys 35(2):115

15. Peters J et al (2008) Relating spectroscopic measurements in a plasma cutting torch to cutting performance. Plasma Chem Plasma Process 28(3):331–352

16. Colombo V et al (2012) Advances in plasma arc cutting technology: the experimental part of an integrated approach. Plasma Chem Plasma Process 32(3):411–426

17. Nemchinsky VA, Severance W (2009) Plasma arc cutting: speed and cut quality. J Phys D Appl Phys 42(19):195204

18. Gonzalez J, Freton P, Masquère M (2007) Experimental quantification in thermal plasma medium of the heat flux transferred to an anode material. J Phys D Appl Phys 40(18):5602

19. Long NP et al (2012) Cathode diameter and operating parameter effects on hafnium cathode evaporation for oxygen plasma cutting arc. J Phys D Appl Phys 45(43):435203

20. Ramakrishnan S et al (2000) Influence of gas composition on plasma arc cutting of mild steel. J Phys D Appl Phys 33(18):2288

21. Adamiak M, Górka J, Kik T (2009) Comparison of abrasion resistance of selected constructional materials. Journal of Achievements in Materials and Manufacturing Engineering 37(2):375–380

22. Camaioni DM, Schwerdtfeger CA (2005) Comment on "accurate experimental values for the free energies of hydration of H+, OH-, and H3O+". J Phys Chem A 109(47):10795–10797

23. Jones G, Fang M (1980) The physics of high-power arcs. Rep Prog Phys 43(12):1415

24. Hrabovsky M (1998) Water-stabilized plasma generators. Pure Appl Chem 70(6):1157–1162

25. Aubrecht V, Bartlova M (2009) Net emission coefficients of radiation in air and SF6 thermal plasmas. Plasma Chem Plasma P 29(2):131–147

26. Bini R et al (2008) Experimental study of the features of the kerf generated by a 200A high tolerance plasma arc cutting system. J Mater Process Tech 196(1):345–355

27. Naghizadeh-Kashani Y, Cressault Y, Gleizes A (2002) Net emission coefficient of air thermal plasmas. J Phys D Appl Phys 35(22):2925